Original Article

The Role of Mesenchymal Stem Cell Derived Exosomes Versus Melatonin on Skin Wound Healing of Adult Male Albino Rats: Histological Study

Dalia Hussein Abdel-Aziz Helmy, Samraa Hussein Abdel Kawi, Amany Mohammed Elsaeed, and Fatma El Zahraa Mohammed Abd El Latif

Department of Medical Histology and Cell Biology, Faculty of Medicine, Beni-Suef University, Egypt.

ABSTRACT

Introduction: Wound healing involves interaction of growth factors and cytokines to restore tissue integrity. Melatonin and MSC-derived exosomes have anti-inflammatory effect, enhance re-epithelization, angiogenesis and regulate collagen remodeling.

Aim of the Work: 28 male albino rats were separated equally into 4 groups: Group I (control) left unwounded. Other groups, full-thickness dermal circular wounds were created. Group II, wound left untreated. Group III (melatonin-treated), melatonin was dissolved in saline and given orally in a dose of 5 mg/kg once daily for 14 days. Group IV (exosomes-treated), exosomes were injected once subcutaneously at four sites around wound at a dose of 200 µg MSC-exosomes in 200 µl PBS. After 14 days, skin sections were examined histologically (by light and electron microscopes). .

Results: Histological and ultrastructural examination of group I was similar to normal skin histological structure. The H&E stained sections from group II indicated a disruption in the outer layer of skin at the wound site, along with a significant presence of inflammatory cells and the new blood vessels formation. Additionally, the masson stained sections revealed thin and disordered collagen fibers in the deeper layer of skin. Electron microscopy analysis of skin slices from group II revealed the absence of hemidesmosomal junctions, along with disruption to the basement membrane and cell-to-cell junctions loss mediated by desmosomes. Both melatonin and MSC-derived exosomes succeeded in restoration of normal histological structure of skin at wound site with more improvement in exosomes treated group .

Conclusion: Melatonin and MSC-derived exosomes have ameliorative effect in skin wound healing.

Received: 06 October 2024, **Accepted:** 19 October 2024

Key Words: Exosomes; Melatonin Skin Wound Healing; Mesenchymal Stem Cell.

Corresponding Author: Amany Mohammed Elsaeed, MSc, Department of Medical Histology and Cell Biology, Faculty of Medicine, Beni-Suef University, Egypt, **Tel.:** +20 01227212188, **E-mail:** amanyyyy2000@gmail.com

ISSN: 1110-0559, Vol. 47, No. 4

INTRODUCTION

The skin, the human body largest tissue, primarily serves to protect the underlying tissues. Wound healing is an intricate method, and effective healing of skin wounds requires a sequence of processes, including inflammation, new tissue production, and remodeling. In addition, the migration, proliferation, differentiation, and death of skin cells play significant roles in this process. The processes involved in this process are carefully coordinated and closely monitored to effectively repair the complex skin structure throughout the regular wound-healing process.[1]

Whether they are acute or chronic, burns, high blood pressure, diabetes, and poor vein flow all result in skin injuries that have a significant impact on society. Healing from wounds is a complex biological process. The technique necessitates the exact collaboration of several cellular entities and the meticulous synchronization of diverse biological and molecular occurrences. There have been few breakthroughs in this field despite significant spending, especially in the treatment of chronic wounds[2]

Melatonin (N-acetyl-5-methoxy-tryptamine) is a hormone that was initially detected in 1959 in the pineal gland and is found throughout the body. It is an inborn substance produced by animals through the pineal gland and other organs and by plants as a secondary metabolite. The human body uses melatonin for a variety of purposes, including mood regulation; sleep regulation, immune system modulation, reproduction, antioxidant protection, and anti-inflammatory effects.[3]

Melatonin, being a lipophilic molecule, is present in almost every tissue in the human body, demonstrating its universal importance. Melatonin has been found to have preventive effects in both normal and abnormal environments. These effects include immune system regulation, cancer suppression, and inflammation reduction. Melatonin has been shown in recent studies to have a positive impact on mucous epithelium and wound healing.[4]

Scientific research has shown a great deal of interest in mesenchymal stem cells (MSCs) due to their easy extraction, extraordinary proliferation power, ability to

DOI: 10.21608/ejh.2024.307534.2111

differentiate into different cell types, and secretion of signaling chemicals. They are a great option for autologous stem cell-based replacement therapy because of these characteristics. MSCs can be easily kept for transit to the treatment site while losing little of their efficacy.[5] MSCs hold great promise for the field of regenerative medicine. Previous studies have demonstrated that MSCs can promote tissue regeneration in a number of organs, including the skin, liver, heart, bone, neural tissue, and cartilage.[6]

The release of extracellular vesicles (EVs) by almost all cell types, including stem cells, is a crucial aspect of intercellular communication.[7] This group includes apoptotic bodies, exosomes, and microvesicles. EVs bind to particular cells through the surface expression of ligands. EVs can carry a wide variety of cargo, including proteins, miRNA, bioactive lipids, and surface receptors.[5]

Exosomes have garnered a lot of attention from scientists in the past few decades. All cell types secrete exosomes, which are tiny membrane vesicles measuring 40-100 nm. Their primary role in cell-to-cell communication is bioactive molecule transfer; they contain nuclear acids, lipids, and proteins. Additionally, exosomes have been implicated in pathophysiology, diagnostics, tissue regeneration, and medication delivery in more recent research. In order to control the behavior and state of the receiving cell, MSCs release exosomes by paracrine signaling. These exosomes carry proteins, RNAs, and lipids. Accelerating wound healing is one function of exosomes produced by MSCs.[1]

MATERIALS AND METHODS

Materials

Chemicals and drugs

Melatonin

Melatonin was obtained from (puritan's pride, Egypt), (CAS. 73-31-4) in the form of tablets, each tablet contained 5 mg of melatonin. The tablet was crushed and dissolved in100 ml saline (CAS. 7647-14-5), so each 1ml of the saline contained 0.05 mg of melatonin. Melatonin was given orally by endogastric tube at a dose of 5mg /kg once per day for 14 days for each animal according to its weight[8]

Exosomes

The PKH-26-labeled exosomes that were produced from mesenchymal stem cells (MSCs-Exos) were donated by the Biochemistry Department of the Faculty of Medicine at Cairo University. Exosomes that had been labeled were put into a syringe after being diluted in 0.5 milliliters of phosphate buffered saline (PBS) (CAS 778-77-0) with PH 7.4. The required dose was 200 µg MSC-exosomes in 200 µl PBS for each rat.[1]

Preparation and isolation of exosomes

Isolation and Preparation of MSCs

In order to obtain bone marrow derived stem cells (BMSCs), the adherent culture method of the complete bone marrow was used on the rabbits' femur and tibia that were four weeks old. The specific cells were grown in a DMEM medium that also contained ten percent fetal bovine serum and one percent penicillin-streptomycin. The cultivation conditions included 37 degrees Celsius temperature and five percent carbon dioxide. The media was replaced every 3 days until the cell culture achieved eighty percent confluency. The cells from the third passage were utilized. BMSCs were characterized utilizing a BriCyte E6 flow cytometer (Mindray DS US Inc., NJ, USA) based on their specific expression of CD44, CD29, CD34 & CD45 markers.[(9]

Preparation of MSCs-Exos

Differential centrifugation is one of the most frequent procedures for exosome purification. To remove cell debris and dead cells, the cell culture supernatants were centrifuged at 300 g for 10 minutes at a temperature of four degrees Celsius, and then at 2,000 g for Ten minutes at four degrees Celsius. The liquid component was centrifuged at a force of 10,000 times the acceleration due to gravity for thirty minutes at a temperature of four degrees Celsius to remove bigger particles. The exosomes were then separated by sedimentation at a temperature of four degrees Celsius using ultracentrifugation at a force of 100,000 times the acceleration because of gravity for seventy minutes. To generate a new pellet, the original pellet was washed with PBS and subsequently centrifuged at a temperature of four degrees Celsius for a length of seventy minutes while applying a force of 100,000 g. The final pellet was dissolved in 200 milliliters of PBS.[10]

Storage of prepared exosomes

Exosomes pellets were stored in deep freezer at -80 ˚C till the intended time of their injection.[1]

Labeling of exosomes

The exosomes were also labeled with PKH-26, a red fluorescent cell linker, using PKH-26 red fluorescent cell linker kits (Sigma, USA, Catalog Number MIN126), in order to label the cell membrane in a broad manner. The PKH-26 dye was diluted in 100 µl of diluent C to obtain a final concentration of 8 µm in the dye solution. Subsequently, a mixture of 10 micrograms of exosomes in 20 microliters of Dulbecco's phosphate-buffered saline (DPBS) (CAS .7647-14-5) was blended with 80 microliters of diluent C. The resultant blend was subsequently introduced into the dye solution and underwent incubation for five minutes, with gentle agitation facilitated by a pipette. Subsequently, the exosomes were combined with one milliliter of DPBS and subjected to ultracentrifugation at a velocity of 100000 ×g for a period of one hour and ten minutes at four degrees Celsius. The pellet was meticulously combined with 50 microliters of DPBS.[12]

Characterization and tracking of MSC-exosomes

In order to analyze the structure of MSCs-exosomes,

the liquid was placed onto copper grids, treated with a 1 percent (w/v) solution of phosphotungstic acid (PTA) (CAS 12501-23-4), and subsequently observed with transmission electron microscopy (TEM).

Menzel-Glaser (Braunschweig, Germany) and Leica Microsystems, Inc. (Buffalo Grove, IL, USA) cryostats were used to generate cryosections of frozen skin, which were then put on SuperFrost® Plus slides. Leica Microsystems CMS GmbH, Wetzlar, Germany's Department of Biochemistry at Cairo University's Faculty of Medicine used a fluorescence microscope to identify fluorescently labeled MSC-EXs in skin cryosections.

Animals

For this research, twenty-eight adult male albino rats ranging in weight from 200 to 250 grams were utilized. The rats were 5 to 6 months old. The Animal House facility at Beni Suef University's Faculty of Pharmacy provided housing for the animals. The room temperature was kept constant among 22 & 24 °C, and each group was housed in its own distinct enclosure. The room's lighting was programmed to follow a 12-hour light-dark cycle, and the animals were free to eat everything they wanted. The rats were provided with a standard commercial pellet diet and were housed for one week prior to the start of the experiment to allow for acclimation. The animals were subjected to the regulations set forth by the animal rights committee (Approval Number 021-157).

Experimental Design

Rats were anesthetized utilizing ether inhalation, and the dorsal hair was shaved under complete aseptic conditions. 1 cm × 1 cm full-thickness dermal circular wounds were created in the skin on the back of the rat using a punch and left uncovered. The animals were separated into four main groups as in (Table 1), 7 rats in each group:

Table 1: All groups

Group	No. of rats	Intervention	Duration
Group I (Control)	7 rats	Left untreated with intact skin	14 days
Group II(wounded, untreated)	7 rats	Skin wound was created (1 cm × 1 cm full-thickness dermal circular wounds) and left untreated and uncovered. Skin specimens were collected at day 14 from wound induction.	14 days
Group III(wounded, melatonin treated)	7 rats	-skin wound was created (1 cm × 1 cm full-thickness dermal circular wounds) - Melatonin was dissolved with saline as mentioned above and given orally by endogastric tube in a dose of 5 mg/k once per day for each rat.	14 days
Group IV (wounded, exosomes treated)	7 rats	-skin wound was created (1 cm × 1 cm full-thickness dermal circular wounds) - MSC-exosomes was injected once subcutaneously at four sites around the wound at a dose of 200 µg MSC-exosomes in 200 µl PBS for each rat.	14 days

Group I (control, non wounded): served as control group and were left unwounded with intact skin,

Group II (wounded, untreated): Skin wound was created as previous and left untreated to heal spontaneously, then rats are sacrificed at day 14 from wound induction and skin specimens are collected from wound site,

Group III (wounded, melatonin treated): skin wound was created as previous. Melatonin was dissolved with saline as mentioned before and given orally by blind ended tube in a dose of 5 mg/kg once per day for 14 days for each animal according to its weight.[8],

Group IV (wounded, exosomes treated): skin wound was created as previous. Mesenchymal stem cell -derived exosomes was injected once subcutaneously at four sites around the wound at a dose of 200 µg MSC-exosomes in 200 µl PBS (phosphate buffer saline) for each rat.[1]

The animals were housed singly (one rat per cage) to avoid scratching each other which would affect the wounding. The day on which the wound was created was designated as day 0. Photographs of the damage site were captured on days 0, 7, and 14, and the size of the wound was measured. A ketamine-xylaine anesthetic was administered to the animals as the experiment came to a close. Full-thickness skin samples, comprising approximately 0.5 cm of the area surrounding the healing lesion, were collected and prepared for histological and ultra-structural studies.

The rats used in the study were simply randomized between groups after stratification for weight.

Histological study

For histological analysis, the skin specimens was perfused and immersed in a fixative solution (10 percent neutral-buffered formalin) for 24 hours, in preparation for paraffin embedding the samples. Slices of 5 µm in thickness were sliced from the blocks and then stained using H&E and Masson's trichrome[13, 14]. The Beni Suef University Faculty of Medicine's Medical Histology and Cell Biology Department conducted the research.

Ultrastructural study

Small sections of skin specimens were fixed for 3

hours at 4Co in 3% glutaraldehyde (CAS No. 111-30-8) in sodium phosphate buffer (Catalog number 6560205) (200 mM, pH 7.2), then postfixed for 1 hour in 1 percent osmium tetroxide (cold) (CAS 20816-12-0). After being dehydrated in ascending sequences of ethanol solutions (70%, 80%, 90%, 95% and 100%) (Cataloge Number 100983) ,the tissue specimens were treated with acetone (Cataloge Number 100014) for 1 hour and then embedded with Araldite. The Leica EM UC6 ultramicrotome was then used to cut and segment the blocks. Picking ultrathin sections (80-100 nm) and staining them with four percent uranyl acetate for 15 minutes and one percent lead citrate for an additional fifteen minutes was done in two separate steps. The grids utilized were 200-mesh Cu. Utilizing an 80 kV transmission electron microscope (Jeol JEM 1011), the stained grids were examined[15]. This research was performed at Mansoura University's Faculty of Agriculture.

Morphometrical study

The data were collected in Faculty of Veterinary Medicine, Beni-Suef University, using an image analyzer computer system Ltd. called the "Leica Qwin 500 C" (Cambridge, England). The video camera was applied to take images of sections under a light microscope in real time, which were then projected onto the screen. Using "Leica Qwin 500 C" software, the image analyzer was controlled by a color video camera, Olympus microscope, a colored monitor, and an IBM personal computer's hard disc that was attached to the microscope. Calibration of the image analyzer was the initial step in having it automatically transform the pixels used as measurement units into micrometers.

The following parameters were calculated

In H&E stained sections, the number of inflammatory cell infiltration was determined by standard high power fields (x 400) in all groups.

The area that represents the percentage of collagen fibers in sections stained with Masson's trichrome, as measured in standard high power fields (x 400) in all groups .

All measurements were performed in 5 high-power fields X400/five different sections of each rat. All these morphometrically measured data were statistically analyzed.

Statistical analysis

Statistical analysis was conducted using statistical package for social sciences (SPSS) software, version 27, IBM, USA. Normal distribution of data was tested using Shapiro Wilk test, while Leven's test was used to test homogeneity of data. Normal distribution and homogeneity of data was violated in all studied parameters (data provided in supplementary data). The data were presented as median and interquartile range (IQR). Non parametric Kruscall Wallis test followed by Bonferoni's posthoc analysis for pairwise comparisons was used to test difference between studied rat groups . Power analysis was done using power analysis tool in SPSS 27 from general linear modeling. These results were confirmed using g*power software version 3.1.9.2., Germany. Power > 0.8 is considered to be acceptable for sample size .

RESULTS

Wound size gross evaluation

At day 0, wounds that were created in group II, III and IV showed redness, with minimal blood oozed out of wound edges that later stopped due to hemostasis. The borders were swollen at the time of wound creation due to inflammation and hemorrhage.

At day 7, the borders of wounds created in

group II were moist and rose with minimal pus formation. A scanty crust formation took place at the borders. On the contrary, the borders of wounds created in

group III and IV were sharp, dry with no abnormality observed. The follow-up of wounds treated with melatonin (group III) & MSC-exosomes

group IV showed that wound healing started few days after injury and evident healing occurred after seven days, with apparent reduction in wound size compared to untreated wounds (group II) as shown in (Figure.1).

At day 14, the wounds of the untreated group (group II) formed a scab over wound site and the total wound size of (groups III & IV) appeared to be lesser than those of untreated group (II) . There was a significant reduction in the wound size in the melatonin & MSC-exosomes groups (III and IV) on day 14 compared to those in the untreated group (II) (Figure 1).

Results of wound size difference between different groups were illustrated in (Table 2) and (Figure.1).

Gp II (Wounded untreated) showed significant larger median wound size (median: 0.59) as compared to normal control group (gp I) (median: 0.00) (*P*: 0.002). Treatment of wounded rats with melatonin (gp III) did not show any significant difference from wounded group (*P*: 0.208). However, treatment of wounded rats with exosome (gp IV) significantly decreased median wound size (median: 0.00) as compared to gp II (median: 0.59) (*P*: 0.024), and it even restored wound size nearly to its normal size (*P*: 1.000). In addition, there was no significant difference between gp III & IV regarding median wound size (medians: 0.16, 0.00, respectively).

II- MSCs – derived exosomes characterization, identification and tracking

TEM images of MSC-EXs showed their spheroid appearance with a diameter below 100 nm.

In group IV (wounded- exosomes treated), PKH labeled MSC- derived exosomes stem cells homed in the wound area (Figure 3). -Histological results

Hematoxylin and Eosin-stained sections

Microscopic analysis of skin section from group I (control group) revealed normal skin histoarchitecture. All skin layers were shown: epidermis, dermis and hypodermis. The epidermis exhibited epidermal rete ridges. The dermis displayed densely arranged, meticulously structured collagen fibers with many hair follicles and sebaceous glands presence, as depicted in(Figure. 4A) and (Figure. 4B). At increased magnification, the epidermis consisted of basal, spiny, granular, and horny layers. The basal cell layer consisted of a single layer of tall columnar cells with pale oval nuclei located at the base. The prickle or spiny cell layer consisted of polyhedral cells that were arranged in multiple layers with centrally located spherical pale nuclei. The cells were separated from one another by narrow gaps. The granular cell layer consisted of spindle-shaped cells with deep basophilic granular cytoplasm. The horny layer consisted of flattened, non-nucleated, keratinized squamous cells. Hair follicle appeared as invagination of epidermis into the dermis (Figure. 4C), (Figure. 4D).

On the other side, skin section from group II (wounded- untreated group) showed histopathological abnormalities in the form of thin creeping epidermis with area of epidermal discontinuity in the wound site, covered with scab. The dermis showed many newly formed blood vessels, areas of hyalinization, many inflammatory cells with no skin appendages (Figure.5A), (Figure.5B), (Figure. 5C) and (Figure.5D).

Treatment of wounded rats with melatonin medication in group III and MSC- exosomes in group IV showed remarkable restoration of the skin histoarchitecture. The skin section from group III, which consisted of wounded individuals treated with melatonin, exhibited a healed wound area with a thin layer of newly formed epidermis. The dermis exhibited recently developed dense collagen bundles, accompanied by a scarcity of inflammatory cells and newly created blood vessels, yet lacking skin appendages (Figure. 6A), (Figure. 6B) &(Figure. 6C) .

The skin section from group IV, which received exosomes treatment, exhibited a thin layer of newly regenerated epidermis that covered the wound site. Observation revealed the presence of recently developed sebaceous glands and hair follicles within the dermis. In (Figure 7A), the dermis exhibited recently developed dense collagen bundles that were oriented in various directions with limited number of recently developed blood vessels and a small number of inflammatory cells (Figure.7B) & (Figure.7C).

Masson's trichrome stained sections

In Masson's trichrome- stained skin sections taken from the control group (I) , collagen bundles were densely packed and well-organized, with sebaceous glands and hair follicles beneath the thick layer of epidermis (Figure. 8A). In contrast, skin sections taken from the wounded-untreated group (II) revealed collagen fibers that were thin and disorganized, stained blue, and had numerous clogged blood vessels. (Figure.8B).

Skin section from group III (wounded- Melatonin treated group) showed thick disorganized collagen bundles in different directions and was covered with continuous layer of epidermis. No skin appendages were seen in dermis (Figure.8C). Skin section from group IV (wounded- Exosomes treated group) showed that the dermis had thick organized collagen bundles in different directions and was covered with continuous epithelial layer. Newly formed skin appendages: hair follicles and sebaceous glands were seen in the dermis (Fig. 8D).

Transmission electron microscopic findings

According to results of the skin ultra-sections groups I control group (unwounded group) , they showed normal ultra-structural layers of epidermis with collagen bundles in different directions in dermis. As regard basal cells, they had euchromatic nucleus with prominent nucleolus and many mitochondria in cytoplasm. They were joined together with desmosomes. They were resting on basement membrane and connected to it with hemidesmosomes. Additionally, the prickle cells were spindle shaped with euchromatic nucleus and prominent nucleolus. They were joined together with desmosomes, so the serrated cell membrane appearance and locations of desmosomes were apparent .There were numerous mitochondria, keratin tonofilament and laminated keratin flakes (Figure. 9).

On the other side, skin ultra-sections of group II (wounded untreated) showed loss the hemidesmosomal junction between epidermal and dermal layer with basement membrane damage. The basal cells displayed shrunken nuclei with widening in intercellular space between them (Figure.10A). There was also a mast cell in dermis in between collagen bundles. It had an eccentric nucleus and multiple electron dense membrane bounded granules filling cytoplasm. (Figure.10B).

Ultrathin sections of Group III and IV demonstrated amelioration in the histopathological alterations detected in group II.

Skin ultra-sections of group III (wounded – melatonin treated) showed all epidermal cell layers. The keratinocytes of basal cell layer had euchromatic nuclei with wide intercellular spaces between each other. They were connected to underlying basement membrane by hemidesmosome with apparent collagen bundles in dermis. The keratinocytes of prickle cell layer displayed euchromatic nuclei. There were widened intercellular junctions with irregularly arranged desmosomes joining cells to each other. The keratinocytes of granular cell layer had keratohyalin granules. Their thick electron dense cell membrane with vesicles was suggesting that lamellar granules were extruding their contents in stratum cornium .There was also a fibroblast which was a spindle shaped cell with oval euchromatic nucleus and prominent nucleolus (Figure.11).

Skin ultra-sections of group IV (wounded – exosomes treated) showed all epidermal cell layers. The keratinocytes of basal cell layer had euchromatic nuclei and connected together with desmosomes.They were connected to underlying basement membrane by hemidesmosomes with apparent collagen bundels in dermis and wide intercellular spaces between each other. The keratinocytes of prickel cell layer were spindle shaped with oval euchromatic nuclei. There was widened intercellular junction with irregularly arranged desmosome to join cells together. The keratinocytes of granular cell layer have keratohyalin granules. Their thick electron dense cell membrane with vesicles was suggesting that lamellar granules are extruding their contents in stratum cornium (Figure.12 A, 12 B and 12 C). There was also a fibroblast which was a spindle shaped cell with oval euchromatic nucleus. There were collagen fibers surrounding it in the dermis in different directions indicating the beginning of fibrous tissue formation beginning on day 14 after onset of wound induction in group IV. (Figure. 12 D).

IV- Morphometric and statistical results

Results of number of inflammatory cells infiltrate difference between different groups were illustrated in (Table 3), (Figure. 13). Gp II (Wounded untreated) showed significant larger median number of inflammatory cell infiltrates (median: 45.00) as compared to normal control group (gp I) (median: 2.00) (*P*<0.001). Treatment of wounded rats with melatonin (gp III) did not show any significant difference from wounded group (*P*: 1.000) regarding median number of inflammatory cells infiltrate. In addition, gp III was still significantly higher than normal rats in terms of median inflammatory cells infiltrate (medians: 33.00, 2.00, respectively) (*P*: 0.044). However, treatment of wounded rats with exosome (gp IV) significantly decreased median number of inflammatory cells infiltrate (median: 20.00) as compared to gp II (median: 45.00) (*P*: 0.044), and it even restored wound size nearly to its normal levels (*P*: 1.000). In addition, there was no significant difference between gp III & IV regarding median number of inflammatory cells infiltrate (medians: 45.00, 33.00, respectively).

Results of % area collagen between different groups were illustrated in (Table 4) , (Figure. 14). Gp II (Wounded untreated) showed significant lower % area collagen (median: 24.17) as compared to normal control group (gp I) (median: 37.12) (*P*: 0.045). Treatment of wounded rats with melatonin (gp III) and exosome (gp IV) significantly increased median % area collagen (median: 45.85, 47.17, respectively) as compared to gp II (median: 24.17) (_: 0.033, 0.001, respectively), and it even restored % area collagen nearly to its normal levels (*P*: 1.000). In addition, there was no significant difference between gp III & IV regarding median % area collagen (median: 45.85, 47.17, respectively).

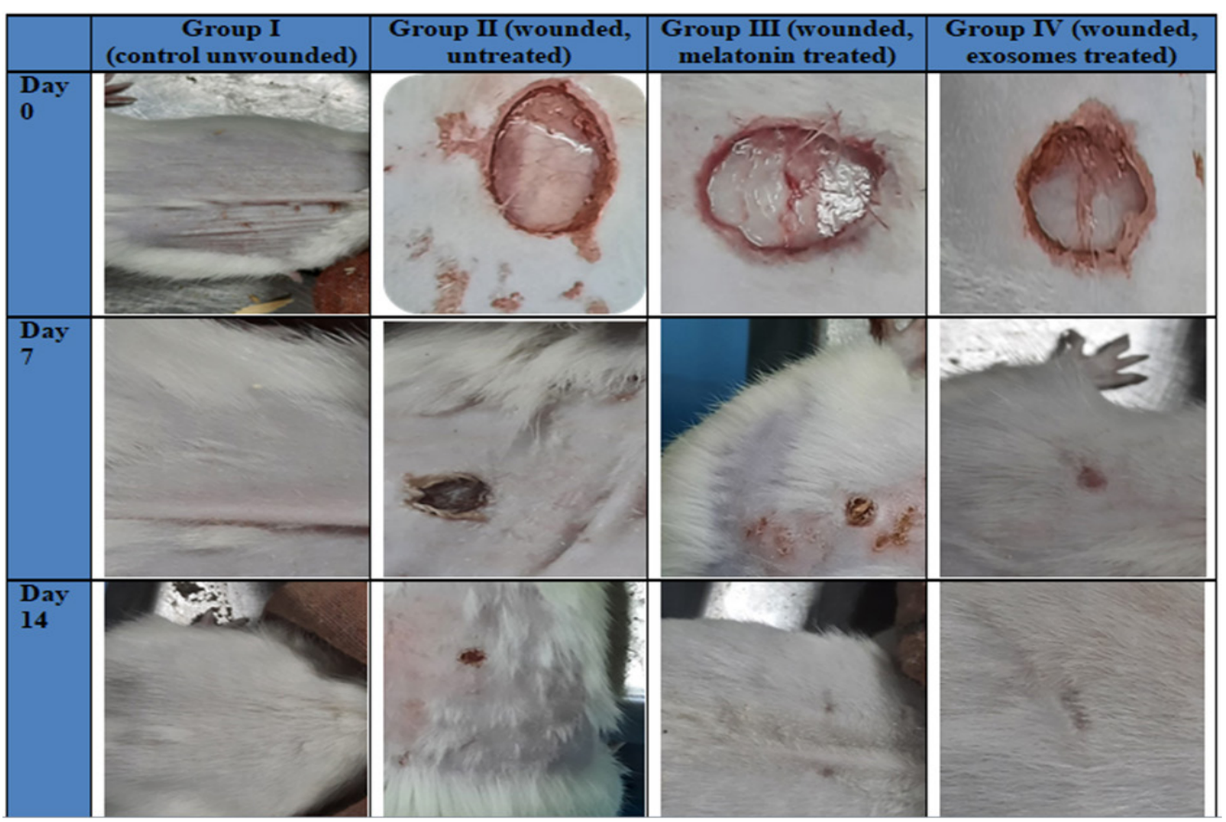

Fig. 1: A photomicrographs showing grossly the wounds of different experimental groups at day0, day7 and day14.

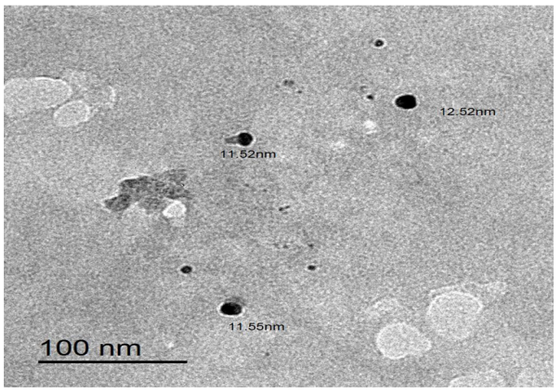

Fig. 2: TEM photomicrograph of MSC- Exosomes

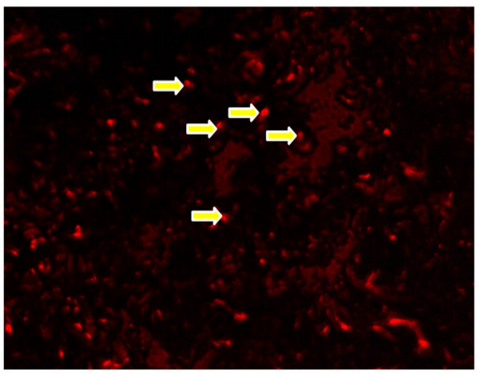

Fig. 3: A photomicrograph of skin section in group IV showing PKH labeled MSC- derived exosomes at wound site (yellow arrows). (PKH X 400)

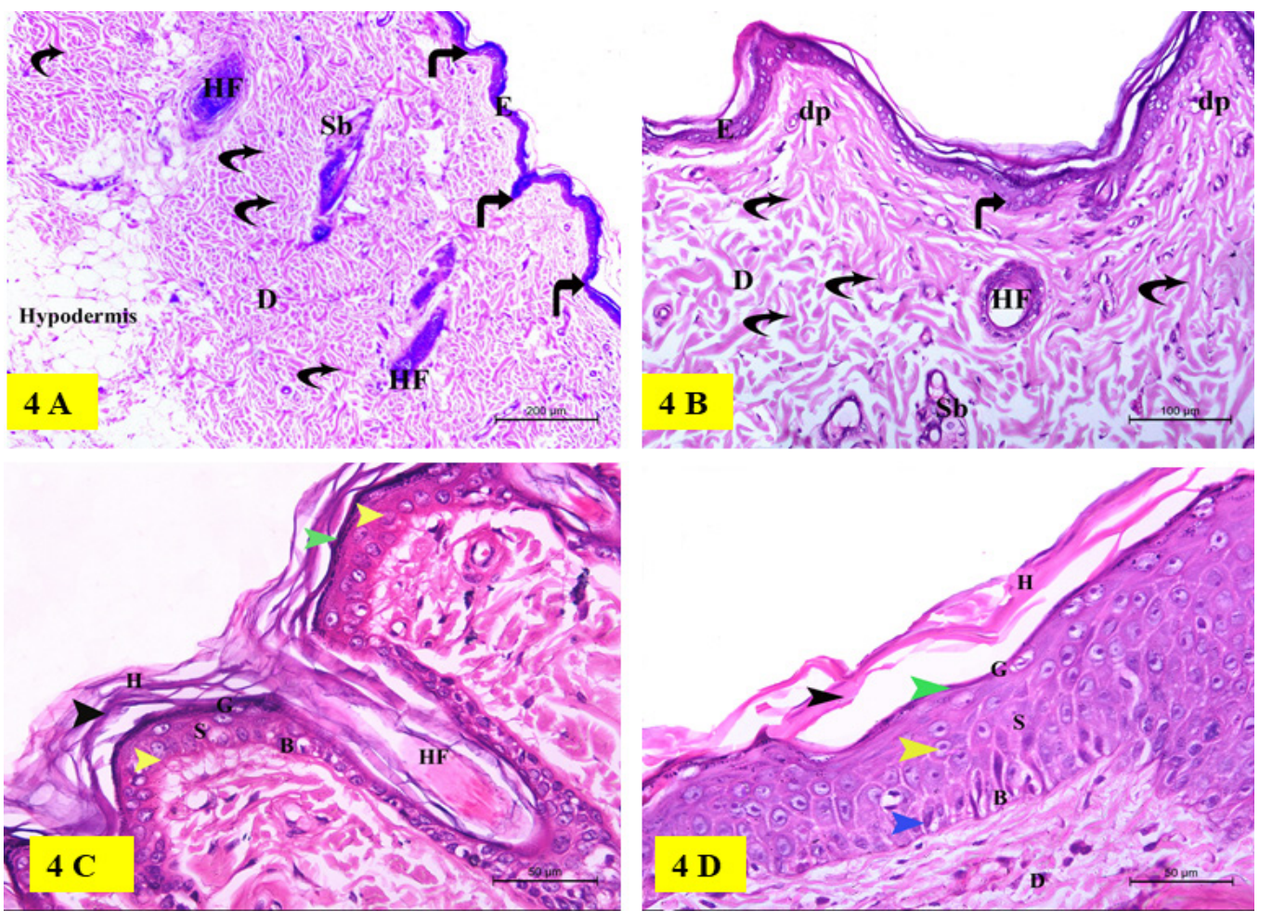

Fig. 4: Photomicrographs of skin sections from group I (control group): **(4A)** shows all skin layers: epidermis (E), dermis (D) and hypodermis. Epidermal rete ridges are seen in the epidermis (E), as indicated by the articulated black arrows. The dermis (D) is characterized by collagen bundles that are densely packed and well organized (shown by curving black arrows). Moreover, there are numerous hair follicles (HF) and sebaceous glands (Sb) that can be observed (H&Ex100) **(4B)** shows a thick epidermis (E) that is characterized by epidermal rete ridges (articulated black arrows). Dermal papillae (dp) are visible in the dermis (D), which is characterized by collagen bundles that are densely packed and well organized (shown by black curved arrows). Additionally, there are numerous hair follicles (HF) and sebaceous glands (Sb) that can be observed (H&Ex200) **(4C)** With higher magnification, the epidermis is formed of basal (B), spiny (S), granular (G) and horny (H) layers. The keratinocytes of basal and spiny layers of keratinocytes have pale nuclei, as indicated by the yellow arrow heads, whereas the granular layer is distinguished by the presence of dark basophilic cytoplasm, as indicated by the green arrow head. The horny layer contains flattened non-nucleated keratinized squamous cells (the black arrow head).Hair follicle (HF) appears as invagination of epidermis into the dermis. (H&Ex400) **(4D)** with higher magnification showing all epidermal layers (basal, prickle, granular and horny layers) and dermis (D). The basal cell layer (B) is formed single layer of tall columnar cells with basal oval pale nuclei (blue arrow head). The prickle or spiny cell layer (S) is formed of more than one layer of polyhedral cells with central rounded pale nuclei (yellow arrow head). The granular cell layer (G) is formed of spindle- shaped cells with deep basophilic granular cytoplasm (green arrow head). The horny layer is formed of flattened non-nucleated keratinized squamous cells (black arrow head).(H&Ex400)

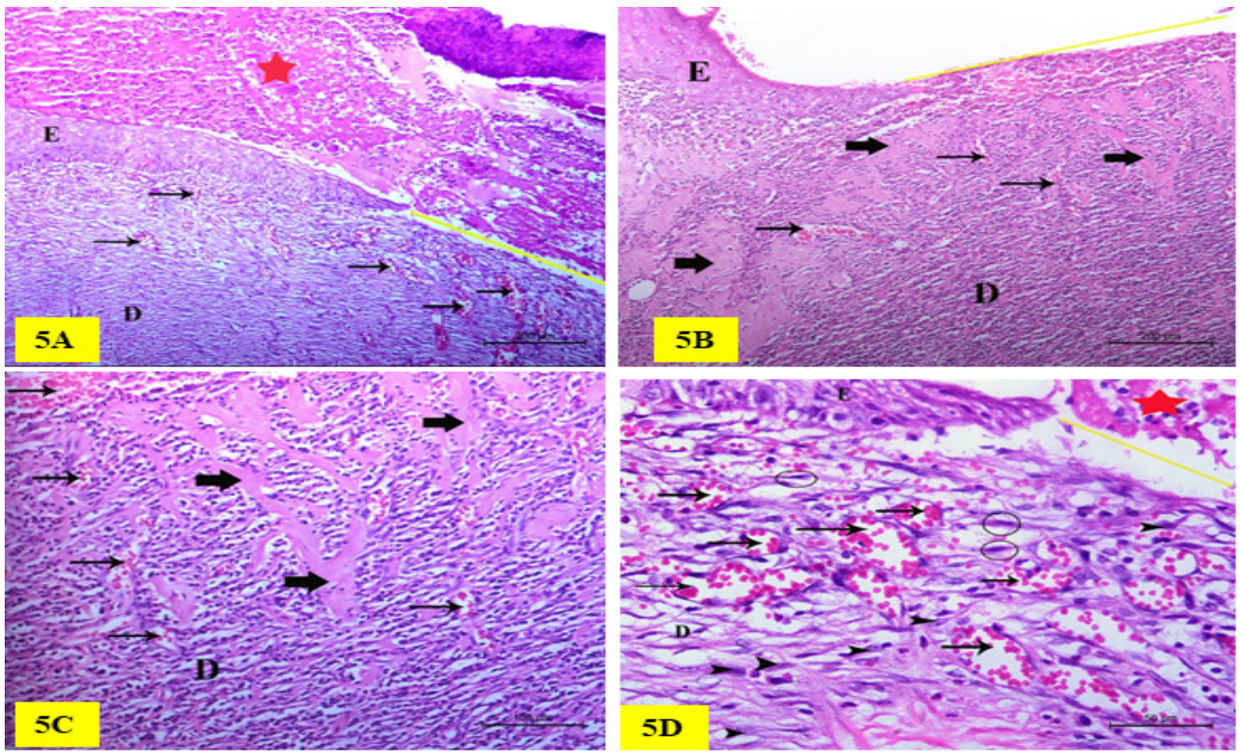

Fig. 5: Photomicrographs of skin sections from group II (wounded- untreated group)**: (5A)** shows thin creeping epidermis (E) with area of epidermal discontinuity (yellow line) in the site of the wound, covered with scab (red star). The dermis (D) shows many newly formed blood vessels (thin arrows). Note the absence of skin appendages. (H&Ex100) **(5B)** shows thin creeping epidermis (E) with area of epidermal discontinuity (yellow line) in the site of the wound. The dermis (D) shows many newly formed blood vessels (thin black arrows) with areas of hyalinization (thick black arrows). Note the absence of skin appendages. (H&Ex100)**(5C)** the dermis (D) shows many newly formed blood vessels (thin black arrows) with areas of hyalinization (thick black arrows). Note the absence of skin appendages.(H&Ex200)**(5D)** with higher magnification, there is thin creeping epidermis (E) with area of epidermal discontinuity (yellow line) in the site of the wound, covered with scab (red star). A large number of newly formed blood vessels (thin black arrows) are seen in the dermis (D), along with a large number of inflammatory cells (black arrow heads) and a small number of collagen fibrils that are overlapped by fibroblasts (black circles).(H&Ex400)

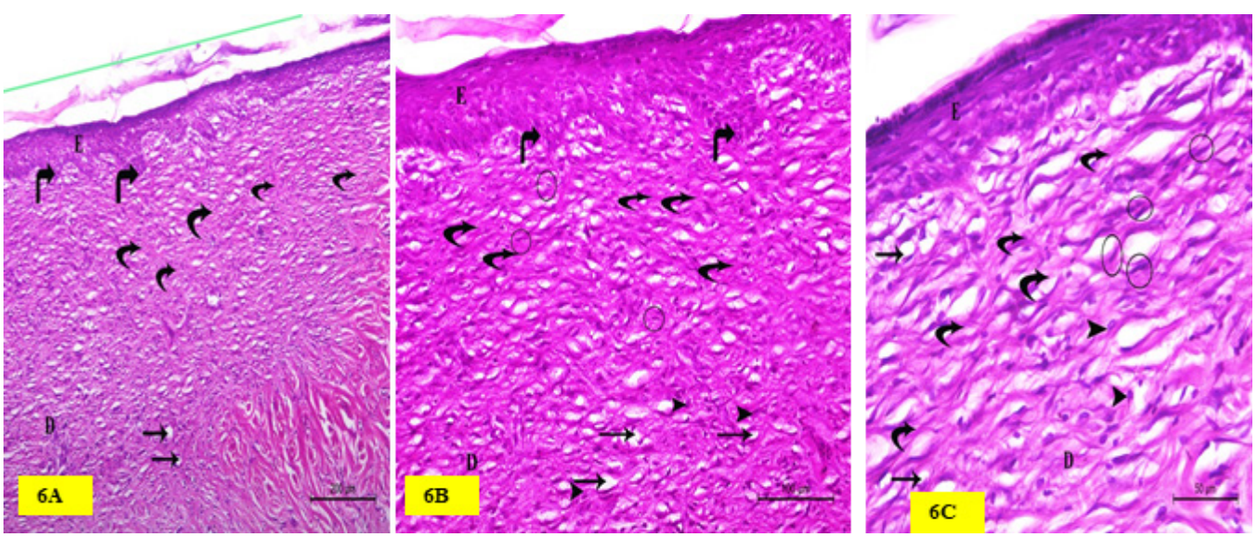

Fig. 6: Photomicrographs of skin sections from group III (wounded- Melatonin treated group):
(6A) shows healed wound area with thin newly formed epidermis (E) and epidermal rete ridges (articulated black arrows). The green line refers to scar area with thin epidermis. The dermis (D) shows newly formed thick collagen bundles (curved black arrows) and few blood vessels (thin black arrows). No skin appendages are seen in the dermis. (H&Ex100) **(6B)** and **(6C):** with higher magnification of the previous section showing healed wound area with thin newly formed epidermis (E) with epidermal rete ridges (articulated black arrows). The dermis (D) shows newly formed thick collagen bundles (curved black arrows) overlapped by fibroblasts (black circles). There are few inflammatory cells (black arrow heads) and few newly formed blood vessels (thin black arrows) in the dermis. Note absence of skin appendages.(H&Ex200) (H&Ex400)

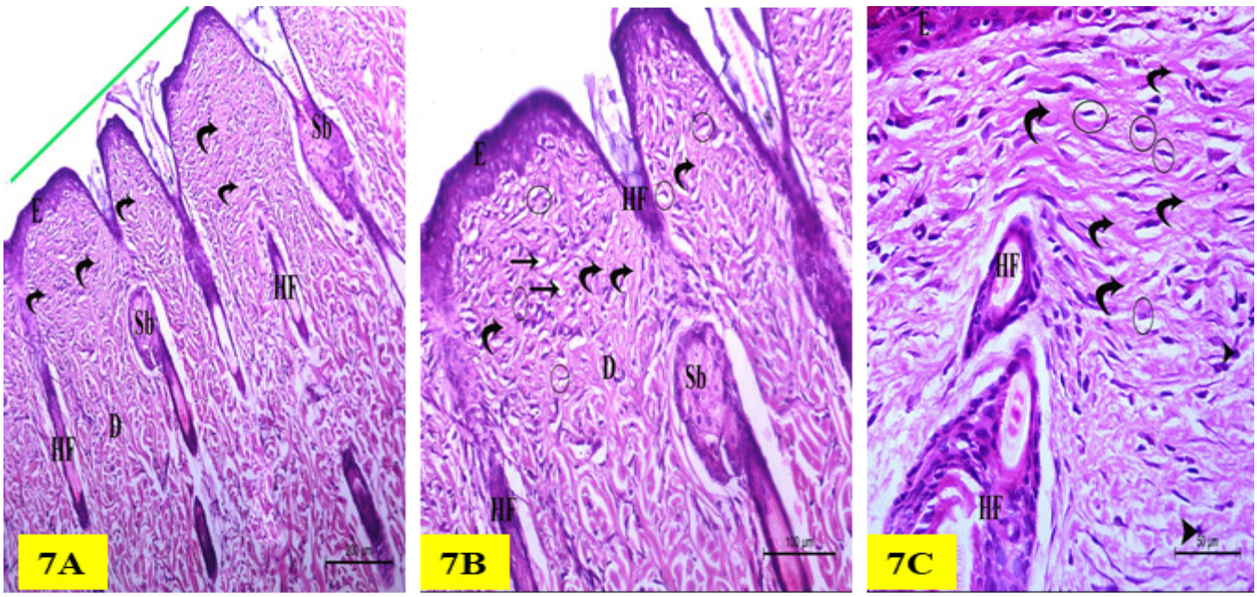

Fig. (7): Photomicrographs of skin sections from group IV (wounded- Exosomes treated group):**(7A)** shows thin newly formed epidermis (E) covering the site of wound healing (green line). Newly formed hair follicles (HF) and sebaceous glands (Sb) are seen in the dermis (D). The dermis also shows newly formed thick collagen bundles (curved arrows) in different directions. (H&Ex100) **(7B)** with higher magnification showing thin newly formed epidermis (E) covering the site of wound healing. Newly formed hair follicles (HF) and sebaceous glands (Sb) are seen in the dermis (D). The dermis also shows newly formed thick collagen bundles (curved black arrows) in different directions overlapped by fibroblasts (black circles), and few newly formed blood vessels (thin black arrows). (H&Ex200) **(7C)** showing site of wound healing where newly formed hair follicles (HF) are formed. There are also newly formed thick collagen bundles (curved black arrows) in different directions overlapped by fibroblasts (black circles) and few inflammatory cells (black arrow heads).(H&Ex400)

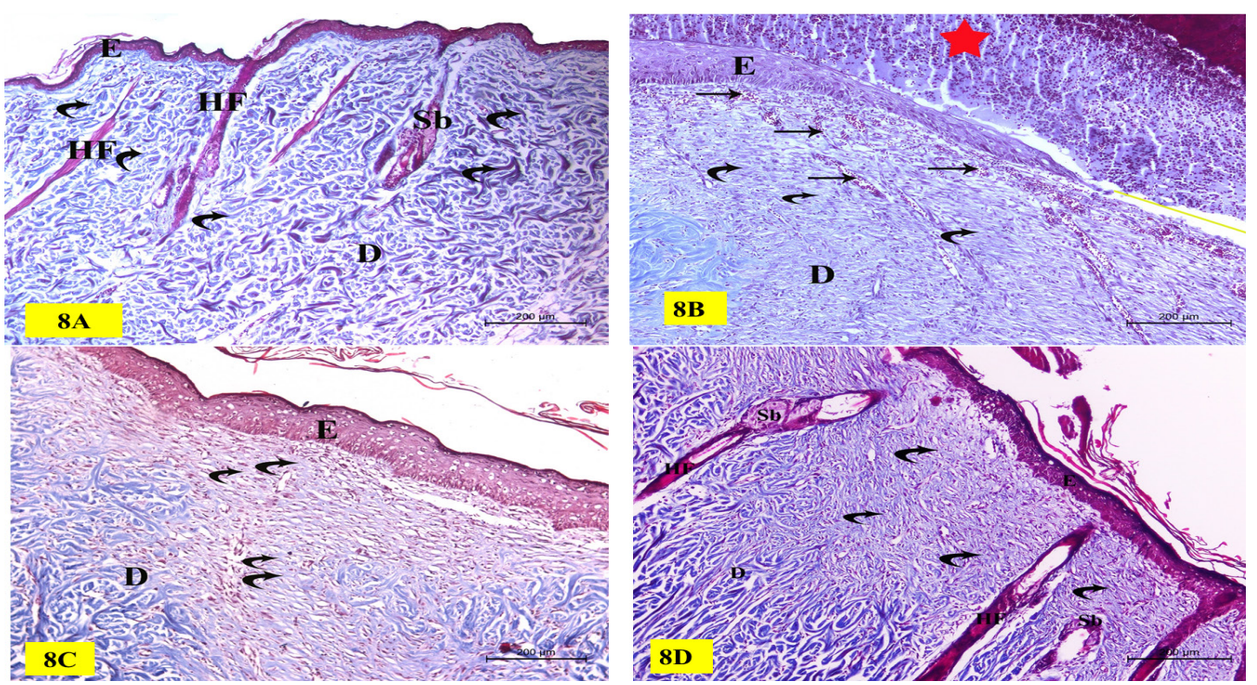

Fig. 8: Photomicrographs of Masson trichrome - stained skin sections**: (8A)** in group I (control group), the dermis (D exhibits tightly packed, well organized collagen bundles (curved black arrows).Additionally, the dermis (D) contains sebaceous glands (Sb) and hair follicles (HF), and it is covered by a thick layer of epidermis (E) **(8B)** In group II (wounded- untreated group), there is thin creeping epidermis (E) over site of wound with an area of epidermal discontinuity (yellow line). Several congested blood vessels (thin black arrows) are visible in the dermis (D), which is characterized by irregularly arranged thin disorganized blue stained collagen fibers (curved black arrows). The wound location is covered by a scab, which is indicated with a red star.**(8C)** In group III (wounded-Melatonin treated group), there are thick disorganized collagen bundles in different directions (curved black arrows) in dermis and is covered with continuous layer of epidermis (E). No skin appendages are seen in dermis (D).**(8D)** In group IV (wounded- Exosomes treated group), the dermis (D) has thick organized collagen bundles in different directions (curved black arrows) and is covered with continuous epithelial layer (E). Newly formed skin appendages: hair follicles (HF) and sebaceous glands (Sb) are seen in the dermis. (Masson's Trichrome x100)

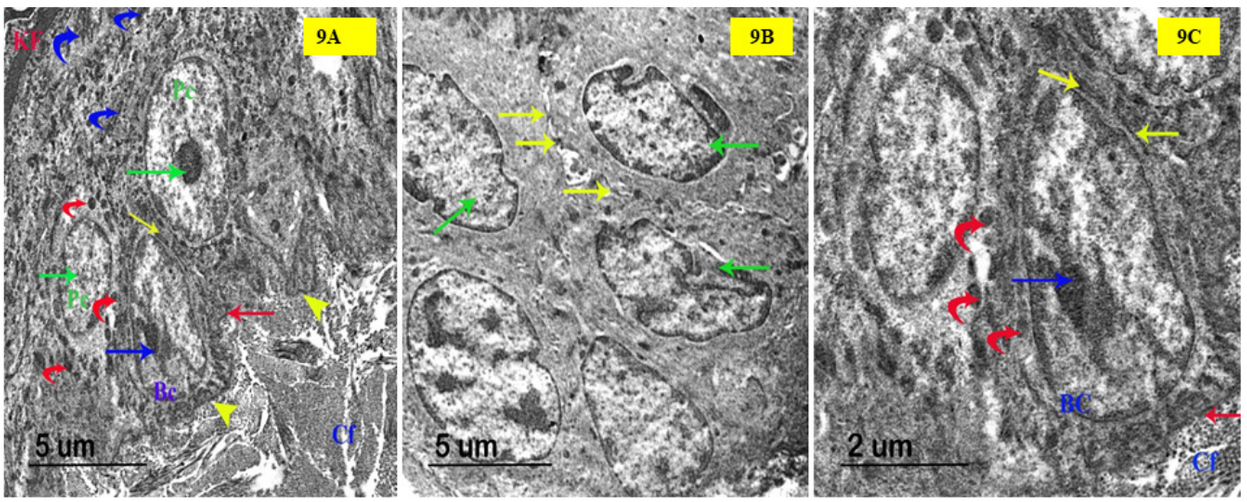

Fig. 9: Transmission electron micrographs of skin sections from group I (control group):**(9A)** showing normal ultra-structural layers of epidermis with collagen bundles (Cf) in different directions in dermis. The basal cell (BC) has euchromatic nucleus and prominent nucleolus (blue arrow),resting on basement membrane (thin red arrow) and connected to it with hemidesmosomes (HD) (yellow arrow heads).The prickle cells (Pc) are spindle shaped with euchromatic nucleus and prominent nucleolus (green arrow).They are joined together with desmosomes (yellow arrow). There are numerous mitochondria (curved red arrow) , keratin tonofilament(curved blue arrow)and laminated keratin flakes (KF). (TEM Scale Bar: 5 µm)**(9B)** showing keratinocyte of prickle cell layer . The prickle cells are spindle shaped with oval euchromatic nuclei (green arrows).The serrated appearance of the cell membrane and locations of desmosomes (yellow arrows) are shown. (TEM Scale Bar: 5 µm) **(9C)** showing keratinocyte of basal cell layer (BC) with collagen bundles (Cf) in dermis. The basal cell has oval euchromatic nucleus with prominent nucleolus (blue arrow) and many mitochondria (curved red arrows). They rest on basement membrane (thin red arrow) .It also shows desmosomes (yellow arrow) to join cells together. (TEM Scale Bar: 2 µm.)

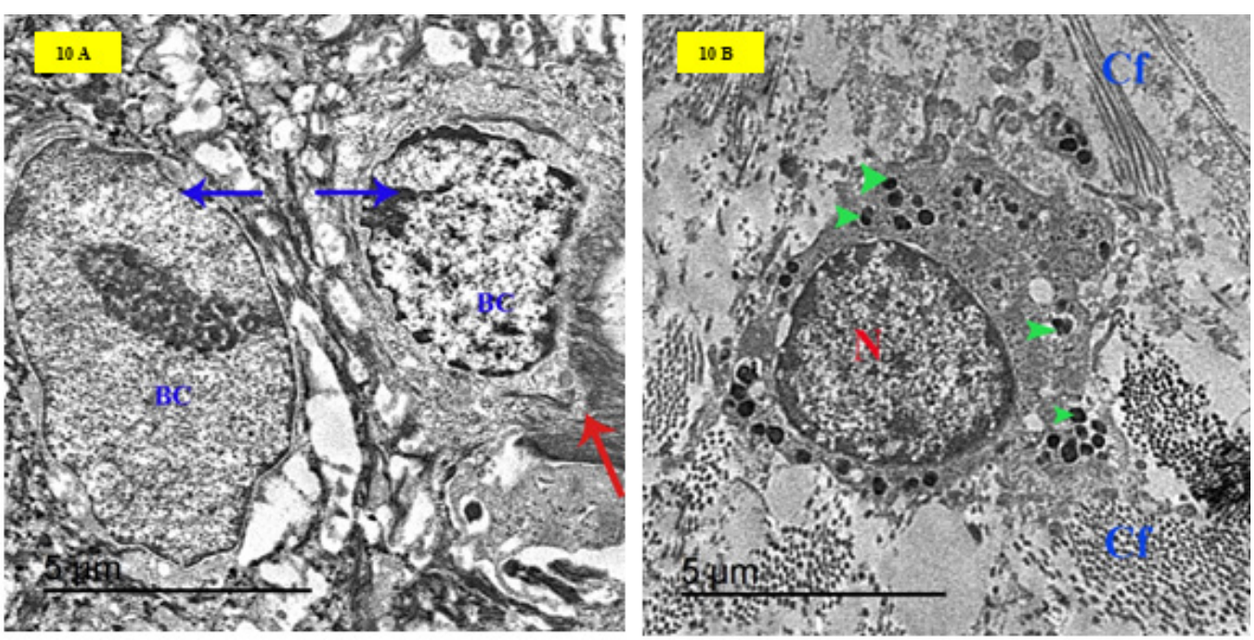

Fig .10 Transmission electron micrographs of skin sections from group II (wounded- untreated group):
(10A): showing loss the hemidesmosomal junction between epidermal and dermal layer with basement membrane damage (red arrow). The basal cells appear to have shrunken nuclei (blue arrows) with widening in intercellular space between them. **(10B):** showing a mast cell in dermis in between collagen bundles. It has an eccentric nucleus (N) and multiple electron dense membrane bounded granules filling cytoplasm (green arrow heads). Both longitudinal and transverse sections of collagen fibers (Cf) are seen. Note the periodicity of collagen fibers. (TEM Scale Bar: 5 µm)

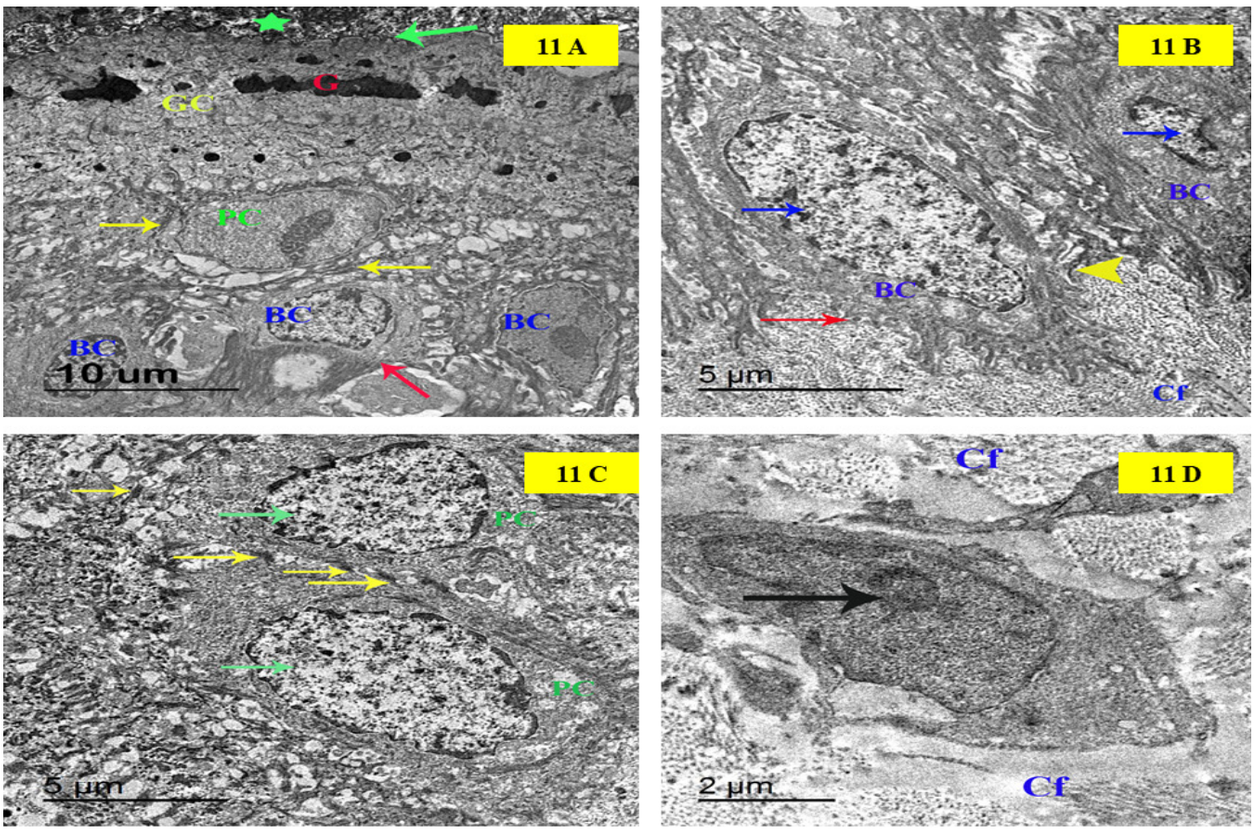

Fig .11 Transmission electron micrographs of skin sections from group III (wounded- Melatonin treated group) :
(11A) :showing all epidermal cell layers .The keratinocytes of basal cell layer (BC) are connected to basement membrane(red arrow) with wide intercellular spaces between each other . The keratinocytes of prickle cell layer (PC) have euchromatic nuclei and connected together with desmosomes (yellow arrows). The keratinocytes of granular cell layer (GC) have keratohyalin granules (G). Their thick electron dense cell membrane (green arrow) with vesicles was suggesting that lamellar granules were extruding their contents in stratum cornium (green star) (TEM Scale Bar: 10 µm)**(11B)** showing the keratinocytes of basal cell layer (BC) with euchromatic nuclei (blue arrows) and widening of the intercellular spaces between each other . They are connected to underlying basement membrane (red arrow) by hemidesmosome (yellow arrow head) with apparent collagen bundles (Cf) in dermis .(TEM Scale Bar: 5 µm) **(11C)** showing the keratinocytes of prickle cell layer (PC) which have euchromatic nuclei (green arrows). There is widened intercellular junction with irregularly arranged desmosome (yellow arrows) to join cells to each other.(TEM Scale Bar: 5 µm) **(11D)** showing a fibroblast . It is a spindle shaped cell with oval euchromatic nucleus and prominent nucleolus (black arrow) .Note the intimate relationship between fibroblast processes with surrounding collagen fibers (Cf). Cross and longitudinal sections of collagen fibers are shown. Note the periodicity of collagen fibers.

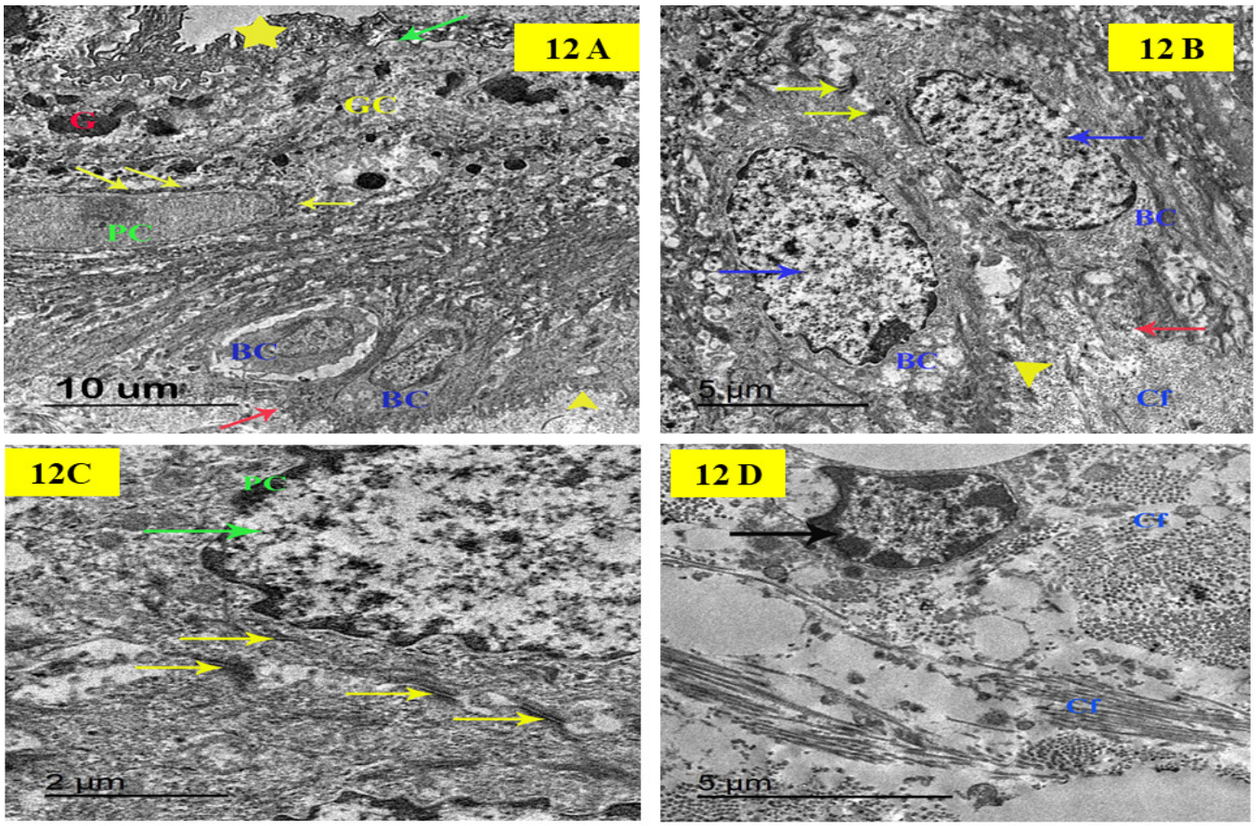

Fig .12 Transmission electron micrographs of skin sections from group IV (wounded- exosomes treated group):
(12A): showing all epidermal cell layers. The keratinocytes of basal cell layer (BC) are connected to basement membrane(red arrow) by hemidesmosomes (yellow arrow head)with wide intercellular spaces between each other . The keratinocytes of prickle cell layer (PC) have oval euchromatic nuclei and connected together with desmosomes (yellow arrows). The keratinocytes of granular cell layer (GC) have keratohyalin granules (G). Their thick electron dense cell membrane (green arrow) with vesicles was suggesting that lamellar granules are extruding their contents in stratum cornium (yellow star).
(TEM Scale Bar: 10 µm)**(12 B):** showing the keratinocytes of basal cell layer (BC) with euchromatic nuclei (blue arrows) and connected together with desmosomes (yellow arrows). They are connected to underlying basement membrane (red arrow) by hemidesmosome (yellow arrow head) with apparent collagen bundles (Cf) in dermis . There is widening of the intercellular spaces between the basal cells.(TEM Scale Bar: 5 µm)**(12C):** showing the keratinocytes of prickle cell layer (PC) which are spindle shaped with oval euchromatic nuclei (green arrows).There is widened intercellular junction with irregularly arranged desmosome (yellow arrows) to join cells together (TEM Scale Bar: 2 µm) **(12D):** showing a fibroblast. It is an oval shaped cell with oval euchromatic nucleus (black arrow) .There are collagen fibers (Cf) surrounding it in the dermis in different directions ,indicating the beginning of fibrous tissue formation beginning on day 14 after onset of wound induction in group IV . Cross and longitudinal sections of collagen fibers are shown. Note the periodicity of collagen fibers. (TEM Scale Bar: 5 µm)

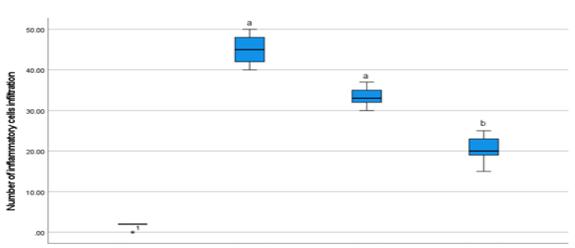

Fig. 13: Box plot graph for median (IQR) inflammatory cell infiltration after 14 days for different experimental groups Data are expressed as median (IQR). Statistical analysis was done using Kruscall Wallis test followed by Bonferoni's posthoc analysis for pairwise comparisons. Group I: Normal control group, Group II: Positive control (wounded untreated) group, Group III: wounded treated with melatonin group, Group IV: wounded treated with exosome group. a: significantly different from gp I at $P<0.05$, b: significantly different from gp II at $P<0.05$, c: significantly different from gp III at $P<0.05$.

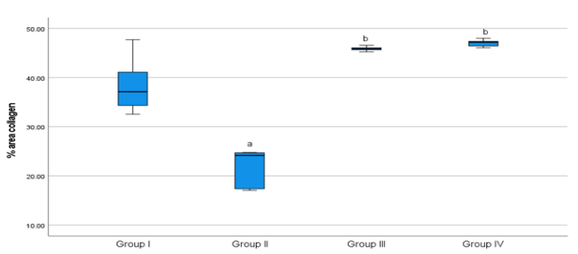

Fig. 14: Box plot graph for median area percent of collagen after 14 days for different experimental groups. Data are expressed as median (IQR). Statistical analysis was done using Kruscall Wallis test followed by Bonferoni's posthoc analysis for pairwise comparisons. Group I: Normal control group, Group II: Positive control (wounded untreated) group, Group III: wounded treated with melatonin group, Group IV: wounded treated with exosome group. a: significantly different from gp I at $P<0.05$, b: significantly different from gp II at $P<0.05$, c: significantly different from gp III at $P<0.05$.

Table 2: Comparison between different studied groups regarding wound size in cm of different experimental groups after 14th days

Studied groups	N	Median (IQR)	KW (df: 3)	*P.value*	Posthoc *P.values*
I	5	0.00 (0.00)	14.355	0.002*	*P*1: 0.002*, P2: 0.872 *P*3: 1.000, P4: 0.208, *P*5: 0.024*, P6: 1.000
II	5	0.59 (0.11)a			
III	5	0.16 (0.20)			
IV	5	0.00 (0.13)b			

Data are expressed as median (IQR). Statistical analysis was done using Kruscall Wallis test followed by Bonferoni's posthoc analysis for pairwise comparisons. KW: test statistics value for Kruscall Wallis test. Df: degree of freedom of the test, N: sample size, gp I: Normal control group, gp II: Positive control (wounded untreated) group, gp III: wounded treated with melatonin group, gp IV: wounded treated with exosome group. *P*1: Posthoc *P.value* for comparison between gp I & II. *P*2: Posthoc *P.value* for comparison between gp I & III. *P*3: Posthoc *P.value* for comparison between gp I & IV. P4: Posthoc *P.value* for comparison between gp II & III. *P*5: Posthoc *P*.value for comparison between gp II & IV. *P6*: Posthoc P.value for comparison between gp III & IV. a: significantly different from gp I at *P*<0.05, b: significantly different from gp II at *P*<0.05, c: significantly different from gp III at *P*<0.05. *: significantly different at *P*<0.05.

Table 3 : Comparison between studied groups regarding number of Inflammatory cell infiltration after 14 days:

Studied groups	N	Median (IQR)	KW (df: 3)	*P.value*	Posthoc *P.value*s
I	5	2.00 (1.00)	17.992	<0.001*	*P*1: <0.001*, P2: 0.044* P3: 1.000, P4: 1.000, P5: 0.044*, P6: 1.000
II	5	45.00 (8.00)a			
III	5	33.00 (5.00)a			
IV	5	20.00 (7.00)b			

Data are expressed as median (IQR). Statistical analysis was done using Kruscall Wallis test followed by Bonferoni's posthoc analysis for pairwise comparisons. KW: test statistics value for Kruscall Wallis test. Df: degree of freedom of the test, N: sample size, gp I: Normal control group, gp II: Positive control (wounded untreated) group, gp III: wounded treated with melatonin group, gp IV: wounded treated with exosome group. *P*1: Posthoc *P.value* for comparison between gp I & II. *P*2: Posthoc *P.value* for comparison between gp I & III. *P*3: Posthoc *P.value* for comparison between gp I & IV. *P*4: Posthoc *P.value* for comparison between gp II & III. *P*5: Posthoc *P.value* for comparison between gp II & IV. *P6*: Posthoc *P.value* for comparison between gp III & IV. a: significantly different from gp I at *P*<0.05, b: significantly different from gp II at *P*<0.05, c: significantly different from gp III at *P*<0.05. *: significantly different at *P*<0.05.

Table 4 : Comparison between studied groups regarding % area collagen fibres after 14 days:

Studied groups	N	Median (IQR)	KW (df: 3)	*P.value*	Posthoc *P.value*s
I	6	37.12 (10.96)	16.458	<0.001*	*P*1: 0.045*, *P*2: 1.000 *P*3: 0.284, *P*4: 0.033*, *P*5: 0.001*, *P*6: 1.000
II	6	24.17 (7.52)a			
III	5	45.85 (0.86)b			
IV	5	47.17 (1.44)b			

Data are expressed as median (IQR). Statistical analysis was done using Kruscall Wallis test followed by Bonferoni's posthoc analysis for pairwise comparisons. KW: test statistics value for Kruscall Wallis test. Df: degree of freedom of the test, N: sample size, gp I: Normal control group, gp II: Positive control (wounded untreated) group, gp III: wounded treated with melatonin group, gp IV: wounded treated with exosome group. *P*1: Posthoc *P.value* for comparison between gp I & II. *P*2: Posthoc *P.value* for comparison between gp I & III. *P*3: Posthoc *P.value* for comparison between gp I & IV. *P*4: Posthoc *P.value* for comparison between gp II & III. *P*5: Posthoc *P.value* for comparison between gp II & IV. *P6*: Posthoc *P.value* for comparison between gp III & IV. a: significantly different from gp I at *P*<0.05, b: significantly different from gp II at *P*<0.05, c: significantly different from gp III at *P*<0.05. *: significantly different at *P*<0.05.

Table 5 : Posthoc power analysis for sample size in different studied parameters:

Studied parameters	N	Partial eta squared	Effect size	Non centrality parameter	Power
Wound size in cm	20	0.970	5.686	520.922	1.000
Number of inflammatory cells infiltrate	20	0.906	3.105	153.751	1.000
% area collagen	22	0.901	3.017	145.349	1.000

Power analysis was done using power analysis tool in SPSS 27 from general linear modeling. These results were confirmed using g*power software. Power > 0.8 is considered to be acceptable for sample size.

DISCUSSION

The skin is the largest organ in terms of surface area in the human body, so it is more susceptible to frequent injury and damage. It is the primary barrier that prevents the damage of interior tissues from environmental hazards such as microbes, UV rays, high temperatures, and mechanical stress [16]. Because of its layered structure and the controlled distribution of various cell types within the extracellular matrix, the regeneration of healthy and functional skin continues to be a huge challenge[17]. The process of skin repair involves a complex sequence of events, including clot formation, proliferation, inflammation and remodeling. The healing process involves the presence of many cytokines and angiogenic agents [18].

Melatonin, generated by numerous sources inside the human body, has a variety of functions, including chronobiological regulation, immunomodulation, drowsiness, tumor suppression, pain reduction, anti-inflammatory action, and antioxidant protection [19]. The use of MSC-exosomes in the repair and therapy of skin wounds has gained popularity. Exosomes are a paracrine component that contributes significantly to the efficacy of stem cells. They are small, single-membrane secretory organelles rich in proteins, lipids, nucleic acids, and carbohydrate conjugates. They may also perform a wide range of other functions, including reorganizing the extracellular matrix and transporting chemicals and messages to neighboring cells. They are stable and easily preserved, which allows for the avoidance of many of the drawbacks associated with stem cells. They also have a homing effect, are not immunologically rejected, and the dosage is easily regulated[20].

Due to the reasons mentioned above, we aimed to assess in the current study the potential protective effect of MSC-exosomes compared to melatonin on the skin wound healing process. We assessed the histological and ultrastructural alterations for this reason to compare their effectiveness.

In the present work, examination of the skin sections by light microscope and transmission electron microscope of group I (control group) did not show substantial differences and their results were similar to the normal structure of skin.

On the other hand, gross examination of the wounds of the untreated group (group II) revealed redness, inflammation and formation of a scab over wound site and the total wound size of (groups III & IV) appeared to be lesser than those of untreated group (II). There was a significant reduction in the wound size in the melatonin & MSC-exosomes groups (III and IV) on day 14 compared to those in the untreated group (II).

The sections of the wounded group stained with H&E (group II) recruited epidermal discontinuity in the site of the wound covered with scab, many newly formed blood vessels, many inflammatory cells infiltration and areas of hyalinization in dermis with no skin appendages. On the contrary, treatment with melatonin & exosomes markedly decreased the wound size & improved the epidermis histological structure. Additioally, the ultrastructural examination showed restoration of the cellular structure along with improved tight junction structure.

In aggrement with our results, Jarad[21] showed that there is granulation tissue formation with inflammatory cell infiltration and new blood vessels formation at the site of wound. Also, Shaygan *et al* [22] revealed that in the negative control group, the majority of the epidermis did not undergo regeneration. The dermis exhibited a dissociated and uneven arrangement with absent appendages, along with a significant infiltration of inflammatory cells. Zhang *et al* [23] reported that H&E staining results of the untreated group revealed the presence of different types of inflammatory cells, a gradual development of granulation tissue, a limited number of collagen fibers and epidermal cells, and a minimal level of epithelialization. In agreement with our results, Albaayit *et al* [24] also detected that incomplete epidermal epithelialization, necrosis, and an overabundance of inflammatory cells in the dermis were observed in the negative control group skin.

In the present study, results of group III (wounded – melatonin treated) and group IV (wounded – exosomes treated) showed that melatonin and exosomes-derived mesenchymal stem cells succeeded in promoting skin wound healing with restoration of almost normal histological skin structure. In addition to that, exosomes-derived mesenchymal stem cells administration showed more ameliorative effect on skin wound healing than bulk melatonin.

Furthermore, H and E stained sections of group III (wounded – melatonin treated) showed thin newly formed epidermis at wound site. The dermis showed few inflammatory cells and few newly formed blood vessels with no skin appendages.

Consistent with what was found in this research, Soriano *et al* [25] detected that melatonin promoted wound healing with reduced infiltration of inflammatory cells when compared with untreated specimens. They attributed that as melatonin has an important role as a potent radical ROS and RNS scavenger (reactive oxygen and nitrogen species). The expression of melatonin receptors in skin cells makes it an optimal candidate for the development of medicines aimed for improving skin cells differentiation and proliferation[26]. Similarly, Mirmajidi *et al* [27]showed that melatonin shown a significant decrease in inflammatory cells. Melatonin promotes wound healing by enhancing new blood vessels formation (angiogenesis) and activating TNF -α (tumor necrosis factor α) ,cytokines, interleukin-1, and the TGF-β1 (transforming growth factor –B) production. Furthermore, it controls specific molecular processes, including inflammation, oxidative stress, and cellular injury.

In the present work, H and E stained sections of group IV (wounded – exosomes treated) revealed thin newly formed epidermis covering the site of wound healing. Newly formed hair follicles and sebaceous glands were seen in the dermis .The dermis also showed newly formed thick collagen bundles in different directions, limited number of recently developed blood vessels and a small number of inflammatory cells. We agreed with, Li *et al* [28] who detected that Exosomes formed from mesenchymal cells effectively decreased the quantity of inflammatory cells, for example, neutrophils and macrophages that infiltrated the tissue, in comparison to the group that did not get any treatment. Exosomes demonstrated anti-inflammatory properties by suppressing the release of pro-inflammatory cytokines & enzymes.

Also Zhang *et al*[(29], Shi *et al* [30] and Tao *et a*l [31] stated that the formation of hair follicles around wounds was completed by exosomes, which aided in the re-epithelialization process during wound healing. Their working hypothesis was that exosomes could speed up the healing process by increasing blood vessel formation at wound locations through enhancing endothelial cell migration and proliferation. Similarly, it were detected by Duan *et al*[32] who reported that Exosomes effectively enhanced the wound healing rate and improved the skin appendage regeneration levels. Additionally, this can be accomplished by suppressing the function of transforming growth factor-β1 (TGF-β1) and its subsequent genes, which play a crucial role in controlling wound healing and tissue regeneration.

Regarding the Masson's trichrome stained skin sections from group II (wounded- untreated group), the dermis exhibited unevenly distributed, thin, and disordered blue-stained collagen fibers, along with numerous congested blood vessels.

Similar results were found by Elbialy *et al*[33] .They detected that there was evidence of immature collagen in the granulation tissues of the untreated control group's skin sections. When healing processes go away, scars form. This can happen when fibroblasts proliferate abnormally or when ECM (Extra cellular matrix) is deposited. Also Basiouny *et al*[34] detected that blue collagen bundles in the reticular dermis that have regenerated are sparse and poorly organized in the wounds of the untreated group.

El Sadik *et al*[35] observed comparable results, as the wound bed of the untreated group exhibited a scarcity of collagen bundles in the regenerated dermis. The collagen bundles had a unidirectional arrangement parallel to the epidermis, but the neighboring healthy skin displayed collagen bundles organized in various directions. Similarly, Shawky *et al*[36] reported that in the untreated group, the wound defect area had collagen bundles that were mildly stained. Collagen is a crucial extracellular matrix component, which has a vital role in maintaining the integrity as well as structure of the skin and other tissues.

In this study, Masson's trichrome stained skin sections of group III (wounded – melatonin treated) showed thick, disorganized collagen bundles in different directions in dermis with no skin appendages. In Chen *et al*[37], Melatonin has been found to decrease iNOS (inducible nitric oxide synthase) levels, increase collagen synthesis and angiogenesis, and speed up wound healing; consequently, the modified Masson staining results showed that the collagen deposition was substantially higher in the melatonin-loaded hydrogel treated group contrasted with the untreated group.

Also, Murali *et al*[38] found that a significant amount of collagen is formed in the group that is treated with melatonin. Melatonin has a role in this since it is an effective antioxidant. Melatonin improved wound healing by lowering malondialdehyde reactive species levels and increasing the production of antioxidant enzymes involving catalases, glutathione reductase, superoxide dismutase, as well as glutathione peroxidase. In addition to its role as an immunomodulator, it impacts angiogenesis, fibroblast proliferation, and monocyte cytokine production[38].

Regarding Masson's trichrome stain, skin slices from group IV (wounded-exosome treated) had dermal thick structured collagen bundles oriented in various orientations, along with newly developed skin appendages such as sebaceous and hair follicles. Li *et al*[28] detected that organized and dense collagen was deposited in the wounds treated with exosomes. Similarly, Liu *et al*[39] stated that exosomes enhanced the growth and movement of mouse fibroblastic cells, leading to a significant increase in the speed of wound healing, faster formation of new epithelial tissue, and higher levels of collagen production. Shi *et al* [30] stated that the exosomes-treated group had a significant accumulation of collagen fibers in the wound bed, arranged in a manner comparable to that of healthy skin.

Transmission electron microscopic skin ultra-sections examination of group II (wounded - untreated) showed that there was loss of the hemidesmosomal junction with basement membrane damage, shrunken nuclei of basal cells with widening in intercellular space between them. The presence of mast cell in dermis suggesting that mast cell proteases mediate damage of desmosomes between keratinocytes.

Similar results were detected by Yassien *et al*[40] who reported that basal columnar cells resting on a discontinuous basement membrane. These cells had irregular nuclei with abundant keratin filaments in the cytoplasm. Also, their cytoplasm contained electron-lucent cytoplasmic vacuoles most probably swollen mitochondria with destroyed cristae. Cells appeared with dilatation of the intercellular spaces and loss of cellular junctions.

These findings suggest that mitochondrial oxidative swelling can cause cytochrome C release and outer mitochondrial membrane rupture, which in turn activates the proapoptotic Bax protein and initiates cell death. Furthermore, the presence of epidermal cells in a fragmented basement membrane may be attributed to apoptosis[41].The expansion of the intercellular spaces and the disruption of cellular connections can be attributed to the disruption of junctions, which is important to reduce the adhesion between cells and facilitate the migration of keratinocytes in an effort to promote healing[42].

Abd-Elhafez *et al*[43] discovered comparable findings, noting the presence of perinuclear gap expansion and irregular dark nuclei with condensed heterochromatin in some keratinocytes. These alterations can be ascribed to ROS (reactive oxygen species) and oxidative stress, which can result in apoptosis. The mitochondria house numerous proteins, one of which is cytochrome C. These proteins have the ability to initiate apoptotic pathways. The formation of the mitochondrial permeability transition pore, a channel, is attributed to ROS. Mitochondrial size increases , and oxidative phosphorylation is interrupted upon channel activation, leading to a slow but steady drop in ATP levels. The increased permeability of the mitochondrial membrane due to its impairment can lead to the release of these proteins into the cytoplasm, ultimately causing cell death[44]. Additionally, there was also an apparent enlargement of the gaps between cells, which can be attributed to the separation of desmosomes and the absence of interaction between adjacent cells[45].

In our study, transmission electron microscopic skin ultra-sections examination of group III (wounded – melatonin treated) showed that the keratinocytes of basal cell layer were connected to basement membrane by hemidesmosome with wide intercellular spaces between each other and keratinocytes of prickle cell layer had euchromatic nuclei and connected together with desmosomes. Consistent with what we found, Mei *et al*[46] reported that melatonin-treated group exhibited a surface epithelial damage attenuation along with improved tight junction structure. Also del Valle Bessone *et al*[47]observed the existence of vacuoles and phagosomes in the cytoplasm, as well as an enlarged inter-lamellar gap between cells in the group treated with melatonin. Therefore, we can infer that the cell death process induced by oxidizing chemicals was reduced due to the anti-inflammatory and antioxidant effects of melatonin.

In our study, transmission electron microscopic skin ultra-sections examination of group IV (wounded – exosomes treated) showed that the keratinocytes of basal cell layer had euchromatic nuclei , connected to basement membrane by hemidesmosomes and connected together with desmosomes. The keratinocytes of prickle cell layer had oval euchromatic nuclei and connected together with desmosomes. The keratinocytes of granular cell layer have keratohyalin granules.

We agreed with Ibrahem *et al*[48] found that in the group treated with exosomes, certain acinar cells exhibited nuclei with loosely packed chromatin (euchromatic nuclei) , along with a substantial number of secretory granules of different sizes that densely occupied the cytoplasm. Additionally, the intercellular junctions remained intact. Also, Salem *et al*[49] and AbuBakr *et al*[50] stated that the group treated with exosomes had acinar seromucous cells with homogenous electron dense secretory granules. The cells also had a normal nucleus located at the base, with obvious nucleoli. Furthermore, the acinar cells had desmosomal connections, which were clearly visible with the presence of intercellular canaliculi.

CONCLUSION

This study demonstrated the anti-inflammatory and wound-healing activity of MSCs – derived exosomes and melatonin, as evidenced by macroscopic, histological,,ultrastructural and morphmetrical analysis. We can infer that each of MSCs – derived exosomes and melatonin act integrally in the wound-healing process, making them a promising alternative to improve the healing process.

This study proved that administration of either MSCs – derived exosomes and melatonin had an accelerating healing effect on the skin wound healing .Moreover, treatment with exosomes was documented with appearance of skin appendages and hair follicles and more organized collagen bundles in the healed wound area than the melatonin treated group.

Further research is needed to elucidate the mechanism of action of MSCs – derived exosomes and melatonin in the wound-healing process. Moreover, evaluations of their effective doses & pharmacokinetic studies are recommended.

RECOMMENDATIONS

1. Clinical trials should be directed to explore whether topical administration of MSCs- derived exosomes have the same regenerative effect in human after further investigations; if so it might be advisable to use MSCs- derived exosomes to rush wound healing & prevent scar formation.
2. Further investigations and studies on combined use of melatonin and MSCs- derived exosomes can be tried on the skin wound as a new strategy to accelerate wound healing and avoid its complications.
3. Additional research is important to investigate the exosomes application produced from MSCs in treating defective wound healing caused by genetic diseases, glucocorticoid therapy, diabetes mellitus, in addition vitamin C insufficiency.

CONFLICT OF INTERESTS

There are no conflicts of interest.

REFERENCES

1. Wang X, Jiao Y, Pan Y, Zhang L, Hongmin Gong H(2019) Fetal dermal mesenchymal stem cell-derived exosomes accelerate cutaneous wound healing by activating notch signaling. Stem cells international, 6(3): 88-100. https://doi.org/10.1155/2019/2402916
2. Ren S, Chen J, Duscher D, Liu Y, Guo G, *et al*.(2019) Microvesicles from human adipose stem cells promote wound healing by optimizing cellular functions via AKT and ERK signaling pathways. Stem Cell Research & Therapy, 10(1): 1-14. https://doi.org/10.1186/s13287-019-1152-x
3. Nabavi SM, Nabavi SF, Sureda A, Xiao J, Dehpour AR, *et al* (2019) Anti-inflammatory effects of Melatonin: A mechanistic review. Critical reviews in food science and nutrition, 59 (1): 4-16. https://doi.org/10.1080/10408398.2018.1487927
4. Jin H, Zhang Z, Wang C, Tang Q, Wang J, *et al* .(2018) Melatonin protects endothelial progenitor cells against AGE-induced apoptosis via autophagy flux stimulation and promotes wound healing in diabetic mice. Experimental & Molecular Medicine, 50 (11): 1-15. https://doi.org/10.1038/s12276-018-0177-z
5. Rostom DM, Attia N, Khalifa HM, Abou Nazel MW, El Sabaawy EA.(2020) The therapeutic potential of extracellular vesicles versus mesenchymal stem cells in liver damage. Tissue Engineering and Regenerative Medicine, 17(6): 537-552. https://doi.org/10.1007/s13770-020-00267-3
6. Alfaifi M, Eom YW, Newsome PN, Baik SK.(2018) Mesenchymal stromal cell therapy for liver diseases. Journal of Hepatology, 68 (6): 1272–1285. https://doi.org/10.1016/j.jhep.2018.01.030
7. Meiliana A, Dewi NM, Wijaya A, etal (2019) Mesenchymal stem cell secretome: Cell-free therapeutic strategy in regenerative medicine. The Indonesian Biomedical Journal,11(2): 113-124. DOI: 10.18585/inabj.v11i2.839
8. Khorsand M, Akmali M, Akhzari M (2019) Efficacy of melatonin in restoring the antioxidant status in the lens of diabetic rats induced by streptozotocin . Journal of Diabetes & Metabolic Disorders, 18 (2): 543-549. https://doi.org/10.1007/s40200-019-00445-8
9. Yao Y, Chen R, Wang G, Zhang Y, Liu F (2019) Exosomes derived from mesenchymal stem cells reverse EMT via TGF-β1/Smad pathway and promote repair of damaged endometrium. Stem Cell Research & Therapy, 10 (5) : 1-17. https://doi.org/10.1186/s13287-019-1332-8.
10. González-Cubero E, González-Fernández ML, Gutiérrez-Velasco L, Navarro-Ramírez E, Villar-Suárez V(2021) Isolation and characterization of exosomes from adipose tissue-derived mesenchymal stem cells. Journal of Anatomy, 238(5): 1203-1217. https://doi.org/10.1111/joa.13365
11. Szatanek R, Baran J, Siedlar M, Baj-Krzyworzeka M. Isolation of extracellular vesicles: Determining the correct approach (2015) International journal of molecular medicine, 36(1): 11-17. https://doi.org/10.3892/ijmm.2015.2194
12. Dominkuš PP, Stenovec M, Sitar S, Lasič E, Zorec R, *et al*(2018) PKH26 labeling of extracellular vesicles: Characterization and cellular internalization of contaminating PKH26 nanoparticles. Biochimica et Biophysica Acta (BBA) Biomembrane , 1860(6): 1350-1361. https://doi.org/10.1016/j.bbamem.2018.03.013
13. Kiernan J (2015) A. Staining with dyes in one or two colours. Histological and Histochemical Methods: Theory and Practice, 5th ed. Kiernan, JA, Ed, 137-169.
14. Bancroft JD, Layton C (2013) Connective and mesenchymal tissues with their stains. Theory and Practice of Histological Techniques. 7th` edition. Churchill Livingstone, Edinburgh, London, Madrid, Melbourne, New York and Tokyo, 200-205.
15. Ayache J, Beaunier L, Boumendil J, Ehret G, Laub D (2010) Sample preparation handbook for transmission electron microscopy: techniques: Springer Science & Business Media, New York, USA.
16. Rodrigues M, Kosaric N, Bonham CA, Gurtner GC (2019) Wound healing: a cellular perspective. Physiological reviews, 99(1): 665-706. doi:10.1152/physrev.00067
17. Pereira, Ruben F., and Paulo J. Bartolo (2016). Traditional therapies for skin wound healing. Advances in wound care .5, (5): 208-229. https://doi.org/10.1089/wound.2013.0506
18. Chen X, Zhou W, Zha K, Liu G, Yang S, *et al*. (2016) Treatment of chronic ulcer in diabetic rats with self-assembling nanofiber gel encapsulated-polydeoxyribonucleotide. American Journal of Translational Research, 8(7): 3067-3076.
19. Ostjen AC, Rosa CGS, Hartmann RM, Schemitt EG, Colares JR, Marroni NP (2019) Anti-inflammatory and antioxidant effect of melatonin on recovery from muscular trauma induced in rats. Experimental and Molecular Pathology, 106(7): 52-59. https://doi.org/10.1016/j.yexmp.2018.12.001
20. An, Yang, Shuyan Lin, Xiaojie Tan, Shiou Zhu, Fangfei Nie, Yonghuan Zhen, Luosha Gu *et al* (2021). Exosomes from adipose-derived stem cells and application to skin wound healing. Cell Proliferation, 54 (3): 12993. https://doi.org/10.1111/cpr.12993
21. Jarad , A(2020) Diabetic wound healing enhancement by tadalafil, 8(5): 50-55. DOI:https://doi.org/10.31838/ijpr/2020.12.03.121

22. Shaygan S, Fakhri S, Bahrami G, Rashidi K, Farzaei MH (2021) Wound-healing potential of Cucurbita moschata Duchesne fruit peel extract in a rat model of excision wound repair. Advances in Pharmacological and Pharmaceutical Sciences, 31(6): 1-8. https://doi.org/10.1155/2021/6697174

23. Zhang L, Liu L, Zhang J, Zhou P (2022) Porcine fibrin sealant promotes skin wound healing in rats. Evidence-Based Complementary and Alternative Medicine, 3(7):112-130. https://doi.org/10.1155/2022/5063625

24. Albaayit SFA, Abba Y, Rasedee A, Abdullah N(2015) Effect of Clausena excavata Burm. f.(Rutaceae) leaf extract on wound healing and antioxidant activity in rats. Drug design, development and therapy, 9(3): 3507-3518. DOI https://doi.org/10.2147/DDDT.S84770

25. Soriano JL, Calpena AC, Rincón M, Pérez N, Halbaut L, *et al*(2020) Melatonin nanogel promotes skin healing response in burn wounds of rats. Nanomedicine, 15(22): 2133-2147. https://doi.org/10.2217/nnm-2020-0193

26. Milan AS, Campmany ACC, Naveros BC (2017) Antioxidant nanoplatforms for dermal delivery: melatonin. Current Drug Metabolism, 18(5): 437–453 .

27. Mirmajidi T, Chogan F, Rezayan AH, Sharifi AM (2021) In *vitro* and in *vivo* evaluation of a nanofiber wound dressing loaded with melatonin. International journal of pharmaceutics, 596(8):120213. https://doi.org/10.1016/j.ijpharm.2021.120213

28. Li M, Wang T, Tian H, Wei G, Zhao L, Shi Y(2019) Macrophage-derived exosomes accelerate wound healing through their anti-inflammation effects in a diabetic rat model. Artificial Cells, Nanomedicine, and Biotechnology, 47 (1): 3793-3803. https://doi.org/10.1080/21691401.2019.1669617

29. Zhang Y, Zhang P, Gao X, Chang L, Chen Z, Mei X (2021) Preparation of exosomes encapsulated nanohydrogel for accelerating wound healing of diabetic rats by promoting angiogenesis. Materials Science and Engineering, 120 (6): 111671. https://doi.org/10.1016/j.msec.2020.111671

30. Shi Q, Qian Z, Liu D, Sun J, Wang X, *et al* (2017) GMSC-derived exosomes combined with a chitosan/silk hydrogel sponge accelerates wound healing in a diabetic rat skin defect model. Frontiers in physiology, 8(7): 904. https://doi.org/10.3389/fphys.2017.00904

31. Tao, SC, Guo SC, Min LI, Ke QF, Guo Y, Zhang CQ (2017) Chitosan wound dressings incorporating exosomes derived from microRNA-126-overexpressing synovium mesenchymal stem cells provide sustained release of exosomes and heal full-thickness skin defects in a diabetic rat model. Stem cells translational medicine, 6(3): 736-747. https://doi.org/10.5966/sctm.2016-0275

32. Duan M, Zhang Y, Zhang H, Meng Y, Qian M, Zhang G (2020) Epidermal stem cell-derived exosomes promote skin regeneration by downregulating transforming growth factor-β1 in wound healing. Stem cell research & therapy, 11(5) : 1-11. https://doi.org/10.1186/s13287-020-01971-6

33. Elbialy ZI, Assar DH, Abdelnaby A, Abu Asa S, Abdelhiee EY, *et al* (2021) Healing potential of Spirulina platensis for skin wounds by modulating bFGF, VEGF, TGF-ß1 and α-SMA genes expression targeting angiogenesis and scar tissue formation in the rat model. Biomedicine & pharmacotherapy, 137(9): 111349. https://doi.org/10.1016/j.biopha.2021.111349

34. Basiouny SH, Salama NM, El Maadawi ZM, Farag EA(2013) Effect of bone marrow derived mesenchymal stem cells on healing of induced full-thickness skin wounds in albino rat. International journal of stem cells, 6(1): 12. doi: 10.15283/ijsc.2013.6.1.12

35. El Sadik AO, El Ghamrawy TA, Abd El-Galil TI (2015) The effect of mesenchymal stem cells and chitosan gel on full thickness skin wound healing in albino rats: histological, immunohistochemical and fluorescent study. PloS one, 10 (9): 0137544. https://doi.org/10.1371/journal.pone.0137544

36. Shawky LM, El Bana EA, Ahmed A. Morsi AA (2019) Stem cells and metformin synergistically promote healing in experimentally induced cutaneous wound injury in diabetic rats. Folia Histochemica et Cytobiologica, 57(3): 127-138. DOI: 10.5603/FHC.a2019.0014

37. Chen K, Tong C, Cong P, Liu Y, Shi X, *et al*(2021) Injectable melatonin-loaded carboxymethyl chitosan (CMCS)-based hydrogel accelerates wound healing by reducing inflammation and promoting angiogenesis and collagen deposition. Journal of Materials Science & Technology, 63(8): 236-245. https://doi.org/10.1016/j.jmst.2020.06.001

38. Murali R, Thanikaivelan P, Cheirmadurai K (2016) Melatonin in functionalized biomimetic constructs promotes rapid tissue regeneration in Wistar albino rats. Journal of Materials Chemistry, 4(35): 5850-5862. https://doi.org/10.1039/C6TB01221C

39. Liu Y, Liu Y, Zhao Y, Wu M, Mao S, *et al* (2022) Application of adipose mesenchymal stem cell-derived exosomes-loaded β-chitin nanofiber hydrogel for wound healing. Folia Histochemica et Cytobiologica, 60 (2): 167-178. DOI: 10.5603/FHC.a2022.0015

40. Yassien, RI, El-Ghazouly DE (2021) The role of hesperidin on healing an incised wound in an experimentally induced diabetic adult male albino rats. Histological and immunohistochemical study. Egyptian Journal of Histology, 44(1): 144-162 DOI: 10.21608/ejh.2020.26334.1263.

41. Al-Hamdany MZ, Al-Hubaity AY, Al-Omary MS (2016) The Histological Changes of the Skin Lesion in Diabetic Foot. Global Journal of Medical Research: C Microbiology and Pathology, 16(1): 200-233.

42. Tan WS, Arulselvan P, Ng SF, Mat Taib CN, Sarian MN, Fakurazi S(2019) Improvement of diabetic wound healing by topical application of Vicenin-2 hydrocolloid film on Sprague Dawley rats. BMC complementary and alternative medicine, 19(1):1-16. https://doi.org/10.1186/s12906-018-2427-y

43. Abd-Elhafez A, Elkelany M, Mousa A, El-deeb T, Adly KA(2021) "The possible curative role of bone marrow-derived mesenchymal stem cells in bleomycin-induced skin changes in adult male albino rats." Egyptian Journal of Histology, 7(5): 120-135. DOI: 10.21608/ejh.2021.80788.1505

44. Kumar V, Abbas A, Fausto N, Mitchell R. Robbins (2007) Basic Pathology. 9th edition. Saunders Elsevier. Philadelphia, (3): 15.

45. Brooke M, Nitoiu D, Kelsel D (2012) Cell–cell connectivity: desmosomes and disease. The Journal of pathology, 226 (2): 158-171. https://doi.org/10.1002/path.3027

46. Mei Q, Diao L, Xu JM, Liu XC, Jin J (2011) A protective effect of melatonin on intestinal permeability is induced by diclofenac via regulation of mitochondrial function in mice. Acta Pharmacologica Sinica, 32(4): 495-502. https://doi.org/10.1038/aps.2010.225

47. del Valle BC, Fajreldines HD, de Barboza GED, de Talamoni NGT, Allemandi DA, *et al* (2019) Protective role of melatonin on retinal ganglion cell: In *vitro* an in *vivo* evidences. Life sciences, 218(7): 233-240. https://doi.org/10.1016/j.lfs.2018.12.053

48. 48. Ibrahem NE, Mekawy NH, Hussein S, Abdel-aziz HM (2023) Therapeutic Role of Salivary Exosomes in Improving Histological and Biochemical Changes Induced by Duct Ligation in the Submandibular Glands of Albino Rats. The Egyptian Journal of Hospital Medicine, 90(1): 308-320. DOI: 10.21608/ejhm.2023.279551

49. Salem, ZA, Kamel AHM, AbuBakr N (2021) Salivary exosomes as a new therapy to ameliorate diabetes mellitus and combat xerostomia and submandibular salivary glands dysfunction in diabetic rats. Journal of Molecular Histology, 52(3): 467-477. https://doi.org/10.1007/s10735-020-09935-z

50. AbuBakr N, Haggag T, Sabry D, Salem ZA (2020) Functional and histological evaluation of bone marrow stem cell-derived exosomes therapy on the submandibular salivary gland of diabetic Albino rats through TGFβ/Smad3 signaling pathway. Heliyon, 6(4): 30-42. https://doi.org/10.1016/j.heliyon.2020.e03789

الملخص العربى

دور الاكسوزومز المشتقة من الخلايا الجذعية الوسيطة مقابل الميلاتونين في التئام جروح الجلد في ذكر الجرذ الابيض البالغ : دراسة هستولوجية

داليا حسين عبد العزيز حلمي، سمراء حسين عبد القوي، أماني محمد السعيد، فاطمة الزهراء محمد عبد اللطيف

قسم الهستولوجيا الطبية وبيولوجيا الخلية، كلية الطب البشري، جامعة بني سويف، مصر

الخلفية: يتضمن التئام الجروح تفاعل عوامل النمو والسيتوكينات لاستعادة سلامة الأنسجة. الميلاتونين والإكسوزومات المشتقة من الخلايا الجذعية الوسيطة لها تأثير مضاد للالتهابات، وتعزز إعادة تكوين النسيج الظهاري، وتكوين الأوعية الدموية، وتنظم إعادة تشكيل الكولاجين.

الهدف من العمل: تقييم تأثير الميلاتونين مقابل الإكسوزومات المشتقة من الخلايا الجذعية الوسيطة في التئام جروح الجلد.

المواد والطرق: تم تقسيم ٢٨ فأراً ذكراً من الجرذان البيضاء بالتساوي إلى ٤ مجموعات: المجموعة الأولى (المجموعة الحاكمة) التي تركت بدون جرح. في المجموعات الأخرى، تم إنشاء جروح دائرية جلدية كاملة السماكة. المجموعة الثانية: ترك الجرح دون علاج. المجموعة الثالثة (المعالجة بالميلاتونين)، تم إذابة الميلاتونين في محلول ملحي وأعطي عن طريق الفم بجرعة ٥ مجم/كجم مرة واحدة يومياً لمدة ١٤ يوماً. المجموعة الرابعة (المعالجة بالإكسوزومات)، تم حقن الإكسوزومات مرة واحدة تحت الجلد في أربعة مواقع حول الجرح بجرعة قدرها ٢٠٠ ميكروجرام من الإكسوزومات المشتقة من الخلايا الجذعية الوسيطة في ٢٠٠ ميكرولتر منPBS. بعد ١٤ يوما، تم فحص مقاطع الجلد تشريحيا (بواسطة المجهر الضوئي والإلكتروني).

النتائج: الفحص النسيجي والبنيوي الدقيق للمجموعة الأولى كان مشابهاً للتركيب النسيجي الطبيعي للجلد. أشارت المقاطع الملونة بالهيماتوكسلين و الايوسين من المجموعة الثانية إلى حدوث خلل في الطبقة الخارجية من الجلد في موقع الجرح، إلى جانب وجود كبير للخلايا الالتهابية وتكوين أوعية دموية جديدة. بالإضافة إلى ذلك، كشفت المقاطع المصبوغة بالماسون عن ألياف كولاجين رقيقة وغير منتظمة في الطبقة العميقة من الجلد. كشف التحليل المجهري الإلكتروني لشرائح الجلد من المجموعة الثانية عن عدم وجود الوصلات الهيمديسوسومية، إلى جانب تعطيل الغشاء القاعدي وفقدان الوصلات من خلية إلى أخرى بواسطة الديسموسومات. نجح كل من الميلاتونين والإكسوزومات المشتقة من الخلايا الجذعية الوسيطة في استعادة البنية النسيجية الطبيعية للجلد في موقع الجرح مع نتائج أفضل في المجموعة المعالجة بالإكسوسومات.

الاستنتاج: الميلاتونين والأكسوزومات المشتقة من الخلايا الجذعية الوسيطة لها تأثيرأفضل في التئام جروح الجلد

الكلمات الدالة: الخلايا الجذعية الوسيطة؛ الاكسوزومات ؛ الميلاتونين ؛التئام الجروح الجلدية.